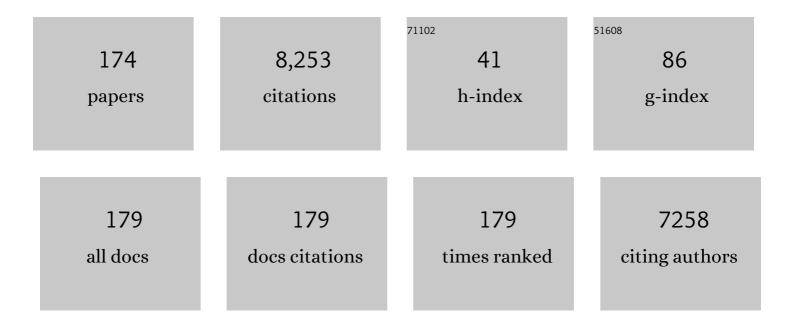
## Peter R Slater

List of Publications by Year in descending order

Source: https://exaly.com/author-pdf/5401583/publications.pdf Version: 2024-02-01



#	Article	IF	CITATIONS
1	Recycling lithium-ion batteries from electric vehicles. Nature, 2019, 575, 75-86.	27.8	1,699
2	Atomic-Scale Investigation of Defects, Dopants, and Lithium Transport in the LiFePO4 Olivine-Type Battery Material. Chemistry of Materials, 2005, 17, 5085-5092.	6.7	966
3	New Chemical Systems for Solid Oxide Fuel Cells. Chemistry of Materials, 2010, 22, 675-690.	6.7	329
4	A combined single crystal neutron/X-ray diffraction and solid-state nuclear magnetic resonance study of the hybrid perovskites CH <sub>3</sub> NH <sub>3</sub> PbX <sub>3</sub> (X = I, Br and Cl). Journal of Materials Chemistry A, 2015, 3, 9298-9307.	10.3	253
5	Defect chemistry and oxygen ion migration in the apatite-type materials La9.33Si6O26 and La8Sr2Si6O26. Journal of Materials Chemistry, 2003, 13, 1956.	6.7	250
6	Developing apatites for solid oxide fuel cells: insight into structural, transport and doping properties. Journal of Materials Chemistry, 2007, 17, 3104.	6.7	239
7	Cooperative mechanisms of fast-ion conduction in gallium-based oxides with tetrahedral moieties. Nature Materials, 2007, 6, 871-875.	27.5	185
8	Synthesis and electrical characterisation of doped perovskite titanates as potential anode materials for solid oxide fuel cells. Journal of Materials Chemistry, 1997, 7, 2495-2498.	6.7	157
9	Development of apatite-type oxide ion conductors. Chemical Record, 2004, 4, 373-384.	5.8	143
10	An apatite for fast oxide ion conductionElectronic supplementary information (ESI) available: interatomic potentials. See http://www.rsc.org/suppdata/cc/b3/b301179h/. Chemical Communications, 2003, , 1486.	4.1	127
11	Solid state 29Si NMR studies of apatite-type oxide ion conductors. Journal of Materials Chemistry, 2006, 16, 1410.	6.7	118
12	Local Defect Structures and Ion Transport Mechanisms in the Oxygen-Excess Apatite La <sub>9.67</sub> (SiO <sub>4</sub> ) <sub>6</sub> O <sub>2.5</sub> . Chemistry of Materials, 2008, 20, 5055-5060.	6.7	115
13	Doping and defect association in AZrO3(A = Ca, Ba) and LaMO3(M = Sc, Ga) perovskite-type ionic conductors. Dalton Transactions, 2004, , 3061.	3.3	106
14	Doping strategies to optimise the oxide ion conductivity in apatite-type ionic conductors. Dalton Transactions, 2004, , 3106.	3.3	96
15	Effect of Ga incorporation on the structure and Li ion conductivity of La3Zr2Li7O12. Dalton Transactions, 2012, 41, 12048.	3.3	96
16	Cation ordering in Li containing garnets: synthesis and structural characterisation of the tetragonal system, Li7La3Sn2O12. Dalton Transactions, 2009, , 5177.	3.3	81
17	Synthesis and conductivities of the apatite-type systems, La9.33+xSi6â^'yMyO26+z (M=Co, Fe, Mn) and La8Mn2Si6O26. lonics, 2002, 8, 149-154.	2.4	78
18	Fluorination of perovskite-related SrFeO3â^î. Solid State Communications, 2005, 134, 621-624.	1.9	76

#	Article	IF	CITATIONS
19	Atomic-scale mechanistic features of oxide ion conduction in apatite-type germanates. Chemical Communications, 2008, , 715-717.	4.1	75
20	A comparison of the effect of rare earth vs Si site doping on the conductivities of apatite-type rare earth silicates. Journal of Solid State Electrochemistry, 2006, 10, 562-568.	2.5	72
21	Effect of oxygen content on the 29Si NMR, Raman spectra and oxide ion conductivity of the apatite series, La8+xSr2â^'x(SiO4)6O2+x/2. Dalton Transactions, 2008, , 5296.	3.3	64
22	Oxyanion doping strategies to enhance the ionic conductivity in Ba <sub>2</sub> In <sub>2</sub> O <sub>5</sub> . Journal of Materials Chemistry, 2011, 21, 874-879.	6.7	63
23	Topochemical modifications of mixed metal oxide compounds by low-temperature fluorination routes. Reviews in Inorganic Chemistry, 2013, 33, 105-117.	4.1	61
24	Neutron diffraction and atomistic simulation studies of Mg doped apatite-type oxide ion conductors. Faraday Discussions, 2007, 134, 181-194.	3.2	59
25	Oxygen Defects and Novel Transport Mechanisms in Apatite Ionic Conductors: Combined <sup>17</sup> Oâ€NMR and Modeling Studies. Angewandte Chemie - International Edition, 2011, 50, 9328-9333.	13.8	57
26	Facile proton conduction in H+/Li+ ion-exchanged garnet-type fast Li-ion conducting Li5La3Nb2O12. Journal of Materials Chemistry A, 2013, 1, 13469.	10.3	57
27	Synthesis and structure of the new oxide fluoride Sr2TiO3F2 from the low temperature fluorination of Sr2TiO4: an example of a staged fluorine substitution/insertion reaction. Journal of Materials Chemistry, 2002, 12, 291-294.	6.7	53
28	Investigation into the effect of Si doping on the performance of SrFeO3â^´Î´SOFC electrode materials. Journal of Materials Chemistry A, 2013, 1, 11834.	10.3	53
29	Synthesis and structural determination of the new oxide fluoride BaFeO2F. Solid State Communications, 2007, 141, 467-470.	1.9	52
30	Large Nonclassical Electrostriction in (Y, Nb)‣tabilized <i>δ</i> â€Bi <sub>2</sub> O <sub>3</sub> . Advanced Functional Materials, 2016, 26, 1138-1142.	14.9	50
31	An investigation of the synthesis and conductivities of La-Ge-O based systems. Ionics, 2002, 8, 155-160.	2.4	49
32	High-Voltage Stabilization of O3-Type Layered Oxide for Sodium-Ion Batteries by Simultaneous Tin Dual Modification. Chemistry of Materials, 2022, 34, 4153-4165.	6.7	47
33	Synthesis and characterisation of the SrxBa1â^'xFeO3â^'y-system and the fluorinated phases SrxBa1â^'xFeO2F. Solid State Sciences, 2010, 12, 1455-1463.	3.2	46
34	Synthesis of silicon doped SrMO3 (M = Mn, Co): stabilization of the cubic perovskite and enhancement in conductivity. Dalton Transactions, 2011, 40, 5599.	3.3	45
35	Enhancement of the conductivity of Ba2In2O5 through phosphate doping. Chemical Communications, 2010, 46, 4613.	4.1	44
36	Structure and magnetic properties of the cubic oxide fluoride BaFeO2F. Journal of Solid State Chemistry, 2011, 184, 1361-1366.	2.9	44

#	Article	IF	CITATIONS
37	Synthesis and characterisation of oxyanion-doped manganites for potential application as SOFC cathodes. Journal of Materials Chemistry, 2012, 22, 8287.	6.7	44
38	Crystallographic and Magnetic Structure of the Perovskite-Type Compound BaFeO <sub>2.5</sub> : Unrivaled Complexity in Oxygen Vacancy Ordering. Inorganic Chemistry, 2014, 53, 5911-5921.	4.0	44
39	A neutron diffraction study of the system Y1-yCayBa2-yLayCu3O7-x. Superconductor Science and Technology, 1992, 5, 205-209.	3.5	42
40	Silicon Doping in Ba <sub>2</sub> In <sub>2</sub> O <sub>5</sub> : Example of a Beneficial Effect of Silicon Incorporation on Oxide Ion/Proton Conductivity. Chemistry of Materials, 2010, 22, 5945-5948.	6.7	42
41	Hydrogen storage and ionic mobility in amide–halide systems. Faraday Discussions, 2011, 151, 271.	3.2	41
42	The structural effects of Na and Ca substitutions on the Y site in YBa2Cu3O7-x. Superconductor Science and Technology, 1989, 2, 5-8.	3.5	40
43	La1â^'xBa1+xGaO4â^'x/2: a novel high temperature proton conductor. Chemical Communications, 2003, , 2694-2695.	4.1	40
44	Combined Experimental and Computational Study of Ce-Doped La <sub>3</sub> Zr <sub>2</sub> Li <sub>7</sub> O <sub>12</sub> Garnet Solid-State Electrolyte. Chemistry of Materials, 2020, 32, 215-223.	6.7	40
45	Analysis of oxyanion (BO 3 3? , CO 3 2? , SO 4 2? , PO 4 3? , SeO 4 4- ) substitution in Y123 compounds studied by X-ray photoelectron spectroscopy. Journal of Superconductivity and Novel Magnetism, 1996, 9, 97-100.	0.5	39
46	Oxyanions in perovskites: from superconductors to solid oxide fuel cells. Dalton Transactions, 2015, 44, 10559-10569.	3.3	39
47	Synthesis and structure of Ba4CaCu2.24O6.96(CO3)0.5, a perovskite containing carbonate anions, and related phases. Journal of Materials Chemistry, 1991, 1, 17.	6.7	37
48	Magnetic order in perovskite-related SrFeO <sub>2</sub> F. Journal of Physics Condensed Matter, 2008, 20, 215207.	1.8	37
49	Development of CaMn <sub>1â<sup>^</sup>x</sub> Ru <sub>x</sub> O <sub>3â<sup>^</sup>y</sub> (x = 0 and 0.15) oxygen reduction catalysts for use in low temperature electrochemical devices containing alkaline electrolytes: ex situ testing using the rotating ring-disk electrode voltammetry method. Journal of Materials Chemistry A. 2014, 2, 3047-3056.	10.3	37
50	Protonic defects and water incorporation in Si and Ge-based apatite ionic conductors. Journal of Materials Chemistry, 2010, 20, 2766.	6.7	36
51	A neutron diffraction study and mode analysis of compounds of the system La1â^'xSrxFeO3â^'xFx (x=1,) Tj ETQq1 206, 158-169.	1 0.7843 2.9	14 rgBT /O 36
52	Structure and Lithium-Ion Dynamics in Fluoride-Doped Cubic Li <sub>7</sub> La <sub>3</sub> Zr <sub>2</sub> O <sub>12</sub> (LLZO) Garnet for Li Solid-State Battery Applications. Journal of Physical Chemistry C, 2018, 122, 27811-27819.	3.1	36
53	Synthesis of oxyanion-doped barium strontium cobalt ferrites: Stabilization of the cubic perovskite and enhancement in conductivity. Journal of Power Sources, 2012, 209, 180-183.	7.8	35
54	Structural studies of apatite-type oxide ion conductors doped with cobalt. Dalton Transactions, 2005, , 1273.	3.3	34

#	Article	IF	CITATIONS
55	Synthesis and electrical characterisation of the perovskite niobate-titanates, Sr1â^'x/2Ti1â^'xNbxO3â^'δ. Ionics, 1996, 2, 213-216.	2.4	33
56	Synthesis and structure of the calcium copper oxyfluoride, Ca2CuO2F2+?. Journal of Materials Chemistry, 1995, 5, 913.	6.7	32
57	Strategies for the Optimisation of the Oxide Ion Conductivities of Apatiteâ€Type Germanates. Fuel Cells, 2011, 11, 10-16.	2.4	32
58	Interaction of (La1â^'xSrx)1â^'yMnO3–Zr1â^'zYzO2â^'d cathodes and LaNi0.6Fe0.4O3 current collecting layers for solid oxide fuel cell application. Solid State Ionics, 2008, 179, 732-739.	2.7	30
59	Raman spectroscopy studies of apatite-type germanate oxide ion conductors: correlation with interstitial oxide ion location and conduction. Journal of Materials Chemistry, 2010, 20, 2170.	6.7	30
60	Topochemical Fluorination of La2NiO4+d: Unprecedented Ordering of Oxide and Fluoride Ions in La2NiO3F2. Inorganic Chemistry, 2018, 57, 6549-6560.	4.0	30
61	Synthesis and structure of the new oxide fluoride Ba2ZrO3F2·xH2O (x â‰^0.5). Journal of Materials Chemistry, 2001, 11, 2035-2038.	6.7	29
62	Apatite germanates doped with tungsten: synthesis, structure, and conductivity. Dalton Transactions, 2011, 40, 3903-3908.	3.3	29
63	Synthesis, structural and magnetic characterisation of the fully fluorinated compound 6H–BaFeO2F. Journal of Solid State Chemistry, 2013, 198, 262-269.	2.9	29
64	Introducing a Large Polar Tetragonal Distortion into Ba-Doped BiFeO <sub>3</sub> by Low-Temperature Fluorination. Inorganic Chemistry, 2014, 53, 12572-12583.	4.0	29
65	Neutron diffraction structural study of the apatite-type oxide ion conductor, La8Y2Ge6O27: location of the interstitial oxide ion site. Journal of Materials Chemistry, 2009, 19, 7955.	6.7	28
66	Synthesis and Characterization of Oxyanionâ€Doped Cobalt Containing Perovskites. Fuel Cells, 2012, 12, 1056-1063.	2.4	28
67	Solid-State Materials for Clean Energy: Insights from Atomic-Scale Modeling. MRS Bulletin, 2009, 34, 935-941.	3.5	27
68	Effect of Ba and Bi doping on the synthesis and sintering of Ge-based apatite phases. Journal of Solid State Electrochemistry, 2004, 8, 668.	2.5	25
69	Synthesis, conductivity and structural aspects of Nd3Zr2Li7â^3xAlxO12. Journal of Materials Chemistry A, 2013, 1, 14013.	10.3	25
70	Anisotropic oxide ion conduction in melilite intermediate temperature electrolytes. Journal of Materials Chemistry A, 2015, 3, 3091-3096.	10.3	25
71	Low temperature fluorination of Sr3Fe2O7â^'x with polyvinylidine fluoride: An X-ray powder diffraction and Mössbauer spectroscopy study. Journal of Solid State Chemistry, 2012, 186, 195-203.	2.9	23
72	Investigation into the effect of Si doping on the performance of Sr1â^'yCayMnO3â^'δ SOFC cathode materials. Dalton Transactions, 2013, 42, 5421.	3.3	23

#	Article	IF	CITATIONS
73	Synthesis, structural and magnetic characterisation of the fluorinated compound 15R-BaFeO2F. Journal of Solid State Chemistry, 2013, 203, 218-226.	2.9	23
74	Thermochemical CO <sub>2</sub> splitting using double perovskite-type Ba <sub>2</sub> Ca <sub>0.66</sub> Nb <sub>1.34â^'x</sub> Fe <sub>x</sub> O <sub>6â^'δ</sub> . Journal of Materials Chemistry A, 2017, 5, 6874-6883.	10.3	23
75	Synthesis and characterization of proton conducting oxyanion doped Ba2Sc2O5. Dalton Transactions, 2012, 41, 261-266.	3.3	22
76	Investigation into the effect of Si doping on the cell symmetry and performance of Sr1â^'yCayFeO3â^'δ SOFC cathode materials. Journal of Solid State Chemistry, 2014, 213, 132-137.	2.9	22
77	Fluorination of the Ruddlesden–Popper type cuprates, Ln2â^'xA1+xCu2O6â^'y (Ln=La, Nd; A=Ca, Sr). Journal of Materials Chemistry, 1997, 7, 2077-2083.	6.7	20
78	An investigation of the high temperature reaction between the apatiteoxide ion conductor La <sub>9.33</sub> Si <sub>6</sub> O <sub>26</sub> and NH3. Journal of Materials Chemistry, 2009, 19, 749-754.	6.7	20
79	Insight into the local structure of barium indate oxide-ion conductors: An X-ray total scattering study. Dalton Transactions, 2012, 41, 50-53.	3.3	19
80	LaNi0.6Co0 4O3â^' dip-coated on Fe–Cr mesh as a composite cathode contact material on intermediate solid oxide fuel cells. Journal of Power Sources, 2014, 269, 509-519.	7.8	19
81	Evaluation of using protective/conductive coating on Fe-22Cr mesh as a composite cathode contact material for intermediate solid oxide fuel cells. International Journal of Hydrogen Energy, 2015, 40, 4804-4818.	7.1	19
82	Topochemical Reduction of La <sub>2</sub> NiO <sub>3</sub> F <sub>2</sub> : The First Ni-Based Ruddlesden–Popper <i>n</i> = 1 T′-Type Structure and the Impact of Reduction on Magnetic Ordering. Chemistry of Materials, 2020, 32, 3160-3179.	6.7	19
83	Electrochemical Reduction and Oxidation of Ruddlesden–Popper-Type La <sub>2</sub> NiO <sub>3</sub> F <sub>2</sub> within Fluoride-Ion Batteries. Chemistry of Materials, 2021, 33, 499-512.	6.7	19
84	Crystallographic Correlations with Anisotropic Oxide Ion Conduction in Aluminum-Doped Neodymium Silicate Apatite Electrolytes. Chemistry of Materials, 2013, 25, 1109-1120.	6.7	18
85	Ionic Conductivity, Structure and Oxide Ion Migration Pathway in Fluorite-Based Bi <sub>8</sub> La <sub>10</sub> O <sub>27</sub> . Chemistry of Materials, 2009, 21, 4661-4668.	6.7	17
86	Low temperature synthesis of garnet solid state electrolytes: Implications on aluminium incorporation in Li7La3Zr2O12. Solid State Ionics, 2020, 350, 115317.	2.7	17
87	Synthesis and characterisation of the perovskite-related cuprate phases YSr2Cu2MO7+y(M = Co, Fe) for potential use as solid oxide fuel cell cathode materials. Journal of Materials Chemistry, 2005, 15, 2321.	6.7	16
88	Fluorination of perovskite-related phases of composition La1â^'xSrxFe1â^'yCoyO3â^'δ. Journal of Physics and Chemistry of Solids, 2008, 69, 2032-2036.	4.0	16
89	Synthesis and structural investigation of a new oxide fluoride of composition Ba2SnO2.5F3·xH2O (xâ‰^0.5). Journal of Solid State Chemistry, 2008, 181, 2185-2190.	2.9	16
90	Preparation of high-oxygen-content apatite silicates through Ti-doping: effect of Ti-doping on the oxide ion conductivity. Journal of Materials Chemistry, 2009, 19, 5003.	6.7	16

#	Article	IF	CITATIONS
91	Synthesis, structural characterisation and proton conduction of two new hydrated phases of barium ferrite BaFeO <sub>2.5â^'x</sub> (OH) <sub>2x</sub> . Journal of Materials Chemistry A, 2016, 4, 3415-3430.	10.3	16
92	Crystal chemistry and optimization of conductivity in 2A, 2M and 2H alkaline earth lanthanum germanate oxyapatite electrolyte polymorphs. Solid State Ionics, 2010, 181, 1189-1196.	2.7	15
93	Novel Aspects of the Conduction Mechanisms of Electrolytes Containing Tetrahedral Moieties. Fuel Cells, 2011, 11, 38-43.	2.4	15
94	La2MgGeO6: a novel Ge based perovskite synthesised under ambient pressure. Chemical Communications, 2002, , 1776-1777.	4.1	14
95	Pseudomorphic 2A→ 2M→ 2H phase transitions in lanthanum strontium germanate electrolyte apatites. Dalton Transactions, 2009, , 8280.	3.3	14
96	Hydrothermal Synthesis, Structure Investigation, and Oxide Ion Conductivity of Mixed Si/Ge-Based Apatite-Type Phases. Inorganic Chemistry, 2014, 53, 4803-4812.	4.0	14
97	Fluorination of perovskite-related phases of composition SrFe1â^'xSnxO3â~δ. Journal of Physics Condensed Matter, 2009, 21, 256001.	1.8	13
98	Effect of tri- and tetravalent metal doping on the electrochemical properties of lanthanum tungstate proton conductors. Dalton Transactions, 2016, 45, 3130-3138.	3.3	13
99	Powder neutron diffraction study of the nasicon-related phases NaxMIIxMIII2 –x(SO4)3 –y(SeO4)y: MII= Mg, MIII= Fe, In. Journal of Materials Chemistry, 1994, 4, 1469-1473.	6.7	12
100	Neutron diffraction structural study of the nasicon-related phases LixMIIxMIII2 –x(SO4)3 –y(SeO4)y(MII= Mg, Ni, Zn; MIII= Al, Cr). Journal of Materials Chemistry, 1994, 4, 1463-1467.	6.7	12
101	Combined experimental and modelling studies of proton conducting La1â^'xBa1+xGaO4â^'x/2: proton location and dopant site selectivity. Journal of Materials Chemistry, 2010, 20, 10412.	6.7	12
102	Battery and solid oxide fuel cell materials. Annual Reports on the Progress of Chemistry Section A, 2012, 108, 424.	0.8	12
103	Laser machining of LaNi0.6M0.4O3â~δ (M: Co, Fe) dip-coated on a Fe–22Cr mesh material to obtain aÂnew contact coating for SOFC: Interaction between Crofer22APU interconnect and La0.6Sr0.4FeO3 cathode. International Journal of Hydrogen Energy, 2015, 40, 8407-8418.	7.1	12
104	Interstitial Oxide Ion Distribution and Transport Mechanism in Aluminum-Doped Neodymium Silicate Apatite Electrolytes. Journal of the American Chemical Society, 2016, 138, 4468-4483.	13.7	12
105	Designing a facile low cost synthesis strategy for the Na–V–S–O systems, NaV(SO <sub>4</sub> ) <sub>2</sub> , Na <sub>3</sub> V(SO <sub>4</sub> ) <sub>3</sub> and Na <sub>2</sub> VO(SO <sub>4</sub> ) <sub>2</sub> . Dalton Transactions, 2018, 47, 13535-13542.	3.3	12
106	Topochemical Fluorination of n = 2 Ruddlesden–Popper Type Sr3Ti2O7 to Sr3Ti2O5F4 and Its Reductive Defluorination. Inorganic Chemistry, 2020, 59, 1153-1163.	4.0	12
107	Raman spectroscopy insights into the α- and δ-phases of formamidinium lead iodide (FAPbI <sub>3</sub> ). Dalton Transactions, 2021, 50, 3315-3323.	3.3	12
108	Cation Distribution and Magnetic Interactions in Substituted Iron-Containing Garnets: Characterization by Iron-57 MA¶ssbauer Spectroscopy. Journal of Solid State Chemistry, 1996, 122, 118-129.	2.9	10

#	Article	lF	CITATIONS
109	X-ray emission and photoelectron spectra, and the location of fluorine atoms in strontium and calcium copper oxyfluorides. Journal of Physics Condensed Matter, 1996, 8, 4847-4854.	1.8	10
110	Local structure investigation of oxide ion and proton defects in Ge-apatites by pair distribution function analysis. Chemical Communications, 2011, 47, 250-252.	4.1	10
111	Reply to "Structural and magnetic behavior of the cubic oxyfluoride SrFeO2F studied by neutron diffraction― Journal of Solid State Chemistry, 2015, 226, 326-331.	2.9	10
112	Synthesis, structure and electrical conductivity of a new perovskite type barium cobaltate BaCoO <sub>1.80</sub> (OH) <sub>0.86</sub> . Dalton Transactions, 2018, 47, 11136-11145.	3.3	10
113	X-ray pair distribution function analysis and electrical and electrochemical properties of cerium doped Li <sub>5</sub> La <sub>3</sub> Nb <sub>2</sub> O <sub>12</sub> garnet solid-state electrolyte. Dalton Transactions, 2020, 49, 11727-11735.	3.3	10
114	Evaluation of the effect of site substitution of Pr doping in the lithium garnet system Li <sub>5</sub> La <sub>3</sub> Nb <sub>2</sub> O <sub>12</sub> . Dalton Transactions, 2020, 49, 10349-10359.	3.3	10
115	High entropy lithium garnets – Testing the compositional flexibility of the lithium garnet system. Journal of Solid State Chemistry, 2022, 308, 122944.	2.9	10
116	Origami: a versatile modeling system for visualising chemical structure and exploring molecular function. Chemistry Education Research and Practice, 2010, 11, 43-47.	2.5	9
117	Exploring the mixed transport properties of sulfur( <scp>vi</scp> )-doped Ba <sub>2</sub> In <sub>2</sub> O <sub>5</sub> for intermediate-temperature electrochemical applications. Journal of Materials Chemistry A, 2016, 4, 11069-11076.	10.3	9
118	Neutron diffraction and multinuclear solid state NMR investigation into the structures of oxide ion conducting La <sub>9.6</sub> Si <sub>6</sub> O <sub>26.4</sub> and La <sub>Si<sub>2</sub>Si<sub>6</sub>O<sub>26</sub>, and their hydrated phases. Dalton Transactions, 2016, 45, 121-133.</sub>	3.3	9
119	Investigation of PO43â^' oxyanion-doping on the properties of CaFe0.4Ti0.6O3â^'î´ for potential application as symmetrical electrodes for SOFCs. Journal of Alloys and Compounds, 2020, 835, 155437.	5.5	9
120	Battery and solid oxide fuel cell materials. Annual Reports on the Progress of Chemistry Section A, 2013, 109, 396.	0.8	8
121	Crystal Chemical Analysis of Nd <sub>9.33</sub> Si <sub>6</sub> O <sub>26</sub> and Nd <sub>8</sub> Sr <sub>2</sub> Si <sub>6</sub> O <sub>26</sub> Apatite Electrolytes Using Aberration-Corrected Scanning Transmission Electron Microscopy and Impedance Spectroscopy. Chemistry of Materials, 2015, 27, 1217-1222.	6.7	8
122	Investigation into the Effect of Sulfate and Borate Incorporation on the Structure and Properties of SrFeO3-δ. Crystals, 2017, 7, 169.	2.2	8
123	The Building Blocks of Battery Technology: Using Modified Tower Block Game Sets to Explain and Aid the Understanding of Rechargeable Li-Ion Batteries. Journal of Chemical Education, 2020, 97, 2231-2237.	2.3	8
124	Oxy-anion substitutions in the system [Y/Ce]2Sr2–xBaxCu3O9–y. Journal of Materials Chemistry, 1993, 3, 1327-1328.	6.7	7
125	Conducting solids. Annual Reports on the Progress of Chemistry Section A, 2010, 106, 429.	0.8	7
126	Structural Study of the Apatite Nd <sub>8</sub> Sr <sub>2</sub> Si <sub>6</sub> O <sub>26</sub> by Laue Neutron Diffraction and Single-Crystal Raman Spectroscopy. Inorganic Chemistry, 2014, 53, 9416-9423.	4.0	7

#	Article	IF	CITATIONS
127	Degradation induced lattice anchoring self-passivation in CsPbI <sub>3â^'x</sub> Br <sub>x</sub> . Journal of Materials Chemistry A, 2020, 8, 9963-9969.	10.3	7
128	Synthesis and conductivity of new lithium-containing Nasicon-type phases: Lix[MxIIM2 –xIII](SO4)3 –y(SeO4)yand Lix[Lix/2M2 –x/2III](SO4)3 –y(SeO4)y. Journal of Materials Chemistry, 1992, 2, 1267-1269.	6.7	6
129	Synthesis and structural characterisation of the new K2NiF4-type phases, A2In0.5Sb0.5O4(A = Sr, Ba). Dalton Transactions, 2005, , 460.	3.3	6
130	24ÂÂConducting solids. Annual Reports on the Progress of Chemistry Section A, 2005, 101, 489.	0.8	6
131	Synthesis and characterisation of vanadium doped alkaline earth lanthanum germanate oxyapatite electrolyte. Journal of Materials Chemistry, 2012, 22, 2658-2669.	6.7	6
132	Investigation into the Incorporation of Phosphate into BaCe1â^'yAyO3â^'y/2 (A = Y, Yb, In). Inorganics, 2014, 2, 16-28.	2.7	6
133	Synthesis and characterization of novel Ge doped Sr 1â^'y Ca y FeO 3â^'δ SOFC cathode materials. Materials Research Bulletin, 2015, 67, 63-69.	5.2	6
134	Magnetic interactions in cubic-, hexagonal- and trigonal-barium iron oxide fluoride, BaFeO <sub>2</sub> F. Journal of Physics Condensed Matter, 2016, 28, 346001.	1.8	6
135	Carbonate: an alternative dopant to stabilize new perovskite phases; synthesis and structure of Ba <sub>3</sub> Yb <sub>2</sub> O <sub>5</sub> CO <sub>3</sub> and related isostructural phases Ba <sub>3</sub> Ln <sub>2</sub> O <sub>5</sub> CO <sub>3</sub> (Ln = Y, Dy, Ho, Er, Tm and Lu). Dalton Transactions. 2018. 47. 12901-12906.	3.3	6
136	Synthesis, structure and electrochemical performance of Eldfellite, NaFe(SO4)2, doped with SeO4, HPO4 and PO3F. Journal of Solid State Chemistry, 2020, 289, 121395.	2.9	6
137	Evaluation of Ga <sub>0.2</sub> Li <sub>6.4</sub> Nd <sub>3</sub> Zr <sub>2</sub> O <sub>12</sub> garnets: exploiting dopant instability to create a mixed conductive interface to reduce interfacial resistance for all solid state batteries. Dalton Transactions, 2021, 50, 13786-13800.	3.3	6
138	Water based synthesis of highly conductive GaxLi7â^'3xLa3Hf2O12 garnets with comparable critical current density to analogous GaxLi7â^'3xLa3Zr2O12 systems. Dalton Transactions, 2021, 50, 2364-2374.	3.3	6
139	Carbon dioxide decomposition through gas exchange in barium calcium iron niobates. Catalysis Today, 2021, 364, 211-219.	4.4	6
140	Structural, Magnetic and Catalytic Properties of a New Vacancy Ordered Perovskite Type Barium Cobaltate BaCoO <sub>2.67</sub> . Chemistry - A European Journal, 2021, 27, 9763-9767.	3.3	6
141	Halogenation of Li <sub>7</sub> La <sub>3</sub> Zr <sub>2</sub> O <sub>12</sub> solid electrolytes: a combined solid-state NMR, computational and electrochemical study. Journal of Materials Chemistry A, 2022, 10, 11172-11185.	10.3	6
142	Dense Oxide Ion Conducting Apatites Prepared by Spark Plasma Sintering. Proceedings of the National Academy of Sciences India Section A - Physical Sciences, 2012, 82, 43-48.	1.2	5
143	A computational study of doped olivine structured Cd <sub>2</sub> GeO <sub>4</sub> : local defect trapping of interstitial oxide ions. Physical Chemistry Chemical Physics, 2016, 18, 26284-26290.	2.8	5
144	Assessing the Importance of Cation Size in the Tetragonalâ€Cubic Phase Transition in Lithiumâ€Garnet Electrolytes**. Chemistry - A European Journal, 2022, 28, .	3.3	5

#	Article	IF	CITATIONS
145	Synthesis of new Mn/Ti containing perovskites and examination of their potential for use as solid oxide fuel cell electrodes. International Journal of Low-Carbon Technologies, 2012, 7, 60-62.	2.6	4
146	On the soft magnetic properties of the compounds of the series NaxMn4.5â^'x/2(VO4)3 and the magnetic structure of h.tMn3(VO4)2 (x = 1). Dalton Transactions, 2013, 42, 7894.	3.3	4
147	Mechanism of Carbon Dioxide and Water Incorporation in Ba2TiO4: A Joint Computational and Experimental Study. Journal of Physical Chemistry C, 2018, 122, 1061-1069.	3.1	4
148	Comparison of the thermal resistance behaviour of synthesized Ln4Al2O9 (Ln = Y, Sm, Eu, Gd, Tb) materials vs commercial Zr0.8Y0.2O1.9 (8YSZ). Surface and Coatings Technology, 2019, 374, 745-751.	4.8	4
149	Introduction of Sulfate to Stabilize the n = 3 Ruddlesden-Popper System Sr4Fe3O10-Î′, as a Potential SOFC Cathode. ECS Transactions, 2019, 91, 1467-1476.	0.5	4
150	Carbon dioxide and water incorporation mechanisms in SrFeO <sub>3â^îr</sub> phases: a computational study. Physical Chemistry Chemical Physics, 2020, 22, 25146-25155.	2.8	4
151	Synthesis and thermal stability of the new copper oxide carbonate Ba4ScCu2O7â^xCO3 and other members of the series Ba4ScxCu2Oy(CO3)2â^x. Journal of Materials Chemistry, 1999, 9, 545-548.	6.7	3
152	Synthesis and electrical characterisation of the apatite-type oxide ion conductors Nd9.33+xSi6-yGayO26+z. lonics, 2004, 10, 353-357.	2.4	3
153	BaCoO <sub>2+Î′</sub> : a new highly oxygen deficient perovskite-related phase with unusual Co coordination obtained by high temperature reaction with short reaction times. Chemical Communications, 2019, 55, 2920-2923.	4.1	3
154	Synthesis of new Ln <sub>4</sub> (Al <sub>2</sub> O <sub>6</sub> F <sub>2</sub> )O <sub>2</sub> (Ln =) Tj ET	Qq0 0 0 r 2.2	gBJ /Overlock
155	Electronic structure of cuprates containing sulfur and phosphorus oxyanions. Physical Review B, 1995, 52, 11830-11836.	3.2	2
156	25  Conducting solids. Annual Reports on the Progress of Chemistry Section A, 2003, 99, 477-504.	0.8	2
157	26 Conducting solids. Annual Reports on the Progress of Chemistry Section A, 2004, 100, 525.	0.8	2
158	Conducting solids. Annual Reports on the Progress of Chemistry Section A, 2006, 102, 482.	0.8	2
159	Conducting solids. Annual Reports on the Progress of Chemistry Section A, 2007, 103, 428.	0.8	2
160	Conducting solids. Annual Reports on the Progress of Chemistry Section A, 2011, 107, 434.	0.8	2
161	Oxygen Migration in Dense Spark Plasma Sintered Aluminumâ€Doped Neodymium Silicate Apatite Electrolytes. Journal of the American Ceramic Society, 2013, 96, 3457-3462.	3.8	2
162	Effect of Si-Doping on the Structure and Conductivity of (Sr/Ca)2MnFeO6-δSystems. ECS Transactions, 2019, 91, 1425-1436.	0.5	2

#	Article	IF	CITATIONS
163	Suitability of strontium and cobalt-free perovskite cathodes with La9.67Si5AlO26 apatite electrolyte for intermediate temperature solid oxide fuel cells. Dalton Transactions, 2020, 49, 14280-14289.	3.3	2
164	Chapter 24. Conducting solids, covering ionic and electronic conductors. Annual Reports on the Progress of Chemistry Section A, 1995, 92, 433.	0.8	1
165	Conducting solids. Annual Reports on the Progress of Chemistry Section A, 2009, 105, 436.	0.8	1
166	Metallic/Ceramic (Fe-22Cr mesh/ LaNi0.6Fe0.4O3-Â) Composite as Contact Material for SOFCs. ECS Transactions, 2015, 68, 1701-1706.	0.5	1
167	Understanding the effect of water transport on the thermal expansion properties of the perovskites BaFe0.6Co0.3Nb0.1O3â^îî´and BaCo0.7Yb0.2Bi0.1O3â^îî´. Journal of Materials Science, 2020, 55, 13590-13604.	3.7	1
168	Chapter 24. Conducting solids, covering ionic and electronic conductors. Annual Reports on the Progress of Chemistry Section A, 1993, 90, 433.	0.8	0
169	Chapter 25. Conducting solids, covering ionic and electronic conductors. Annual Reports on the Progress of Chemistry Section A, 1994, 91, 467.	0.8	0
170	The Synthesis and Characterisation of Ge Containing Apatite-Type Oxide Ion Conductors. Materials Research Society Symposia Proceedings, 2002, 756, 1.	0.1	0
171	26  Conducting solids. Annual Reports on the Progress of Chemistry Section A, 2002, 98, 505-529.	0.8	0
172	Conducting solids. Annual Reports on the Progress of Chemistry Section A, 2008, 104, 414.	0.8	0
173	Synthesis and structure of the perovskite related Sr4-xBaxNa1-yLiy(BO3)3 solid solution series and the related a site cation ordered (Sr/Ca)4Li(BO3)3 system. Journal of Solid State Chemistry, 2021, 294, 121870.	2.9	0
174	Perovskite-Related Oxide Fluorides: The Use of Mössbauer Spectroscopy in the Investigation of Magnetic Properties. Croatica Chemica Acta, 2015, 88, 339-346.	0.4	0